

POISSON LOCAL COLOR CORRECTION FOR IMAGE STITCHING

Mohammad Amin Sadeghi, Seyyed Mohammad Mohsen Hejrati and Niloofar Gheissari

Computer Vision Group, School of Mathematics

Institute for studies in theoretical Physics and Mathematics, Tehran, Iran

Keywords: Image stitching, Poisson equation, Panorama, Color correction, Registration, Image mosaicing.

Abstract: A new method for seamless image stitching is presented. The proposed algorithm is a hybrid method which uses optimal seam methods and smoothes the intensity transition between two images by color correction. A dynamic programming algorithm that finds an optimal seam along which gradient disparities are minimized is used. A modification of Poisson image editing is utilized to correct color differences between two images. Different boundary conditions for the Poisson equation were investigated and tested, and mixed boundary conditions generated the most accurate results. To evaluate and compare the proposed method with competing ones, a large image database consisting of more than two hundred image pairs was created. The test image pairs are taken at different lighting conditions, scene geometries and camera positions. On this database the proposed approach tested favorably as compared to standard methods and has shown to be very effective in producing visually acceptable images.

1 INTRODUCTION

Since two registered images usually have local and global intensity differences, in order to create visually acceptable images it is essential to complement the registration process with seamless image stitching. As noted in (Hasler and Susstrunk, 2000), several factors reflect the intensities recorded by cameras. They include: exposure variances, white balancing, gamma correction, vignetting and digitizer parameters. Seamless stitching has important applications in many high level tasks such as building panoramic images, virtual reality, super resolution and texture synthesis. Recently there have been many breakthrough attempts in seamless image stitching such as (Levin et al., 2003), (Uyttendaele et al., 2001), (Jia and Tang, 2005a), (Jia and Tang, 2005b).

There are two main approaches for the elimination of seams and artifacts in the overlapping images. The first approach is to find an optimal seam along which some energy function is minimized (Jia and Tang, 2005a), (Agarwala et al., 2004). Jia and Tang (Jia and Tang, 2005a) have described different possible energy functions (weighting functions) that might be used to find the optimal seam. These energy functions may be based on intensity or gradient differences of the two images. Dynamic programming or graph cut is

used to minimize the energy function. One advantage of optimal seam methods is that they are applicable to dynamic scenes. This is because the optimal seam does not pass through areas of high gradient disparity. However, optimal seam algorithms are less suitable when the illuminations of the input images are not the same or their overlapping area consists of thin strips.

The second approach is based on enhancing the intensity values of one or both images so that the resulting stitched image looks natural. This task can be performed either globally or locally.

Szeliski and Shum (Shum and Szeliski, 2001) propose a method for building panoramic images capable of correcting local and global intensity misalignments. Their feathering algorithm results in more natural blending effects. Still in many cases it produces unnatural seams under different illumination conditions. Belt and Adelson (Burt and Adelson, 1983) use multiresolution splines for color correction. Uyttendaele et al. (Uyttendaele et al., 2001) proposed a method capable of stitching multiple images taken at various exposures and illuminance conditions. They allow for large scene changes or misregistrations between two images. Levin et al. (Levin et al., 2003) introduced Gradient Domain Image Stitching (GIST) method. GIST utilizes an optimization algorithm to minimize a cost function over image derivatives.

This cost function is a dissimilarity measure between the derivatives of the resulting stitched image and the derivatives of the input images. Jia and Tang (Jia and Tang, 2005b) proposed a tensor voting method for global and local intensity alignment. They use a symmetric tensor representation to model the joint image space (source image and target image intensities) as a token. They extract curves in the image and let tokens on a curve communicate mutually to reinforce each other. A dense tensor field postulates smooth connections among tokens and ensures natural color transitions. This method can successfully handle occlusion and motion blur. Their local intensity alignment approaches is devised to correct vignetting effects.

We have observed that a hybrid method that can take advantage of the strengths of both main approaches, generates more reliable results. Therefore the proposed hybrid method first finds an optimal seam to stitch two images. Then it uses the Poisson equation with mixed boundary conditions in the color domain. As a result, the local color differences between two images are corrected. Poisson equation has been already used for image editing (Pérez et al., 2003) or correcting structure misalignments produced by stitching (Jia and Tang, 2005a). An advantage of the proposed method is its low computational time that makes it particularly desirable for applications to high resolution images. The proposed method relies on a model based registration algorithm to align two images (Gheissari et al., 2008). In fact, the registration algorithm computes the transformation parameters after recovering the transformation model.

This paper is organized as follows: Section 2, gives a brief summary of the registration method used. Methods for finding optimal cutting curve are described in section 3. In section 4, the proposed method, Poisson Local Color Correction (PLCC) is explained. Different boundary conditions for the solution of the Poisson equation are described in the following section (4). Some challenging images for local color correction and the results of applying the proposed algorithm on them are shown in the section 5.

2 MODEL-BASED IMAGE REGISTRATION

In this work, a registration method introduced in (Gheissari et al., 2008) is utilized. In summary this registration method first finds a set of SIFT interest points (Lowe, 1999) and the correspondences between them. The outliers are eliminated to generate an outlier-free set of correspondences. This is

achieved by robustly fitting a translation model to the correspondences. Next all models in the model library are fitted to the above set of inliers.

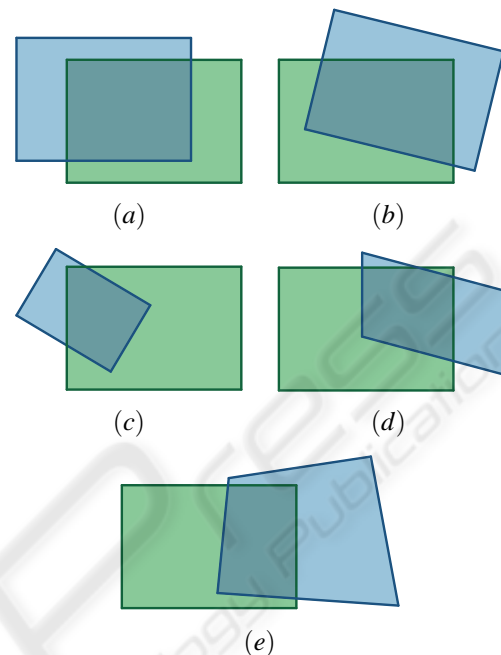


Figure 1: Different transformation models for registration: (a) Translation, (b) Euclidian (c) Similarity, (d) Affine and (e) Projective transformation.

CAIC is applied to select the correct transformation model from a library of candidate models (Bozdogan, 1987). Figure 1 shows the set of candidate models. The final set of inliers is determined by applying the chosen model to the data set. The algorithm estimates the parameters of the chosen model (based on the set of inliers) to generate the transformation matrix.

Before finding the optimal seam and using the Poisson equation to correct color difference, we apply the transformation matrix to the source image. This results in two registered images with an overlapping area which can be a triangle, a rectangle, or a higher order polygon depending on the transformation model.

3 OPTIMAL SEAM METHODS

Optimal seam algorithms are used widely in applications such as pattern synthesis and image stitching (Kwatra et al., 2003), (Jia and Tang, 2005a), (Uyttendaele et al., 2001). These methods find a cutting curve in the overlapping area and stitch the images

along the cutting curve as their common boundary. The main approach in optimal seam algorithms is to specify a weight for each pixel belonging to the overlapping area. Then a curve that minimizes this weight function is selected as the optimal cutting seam.

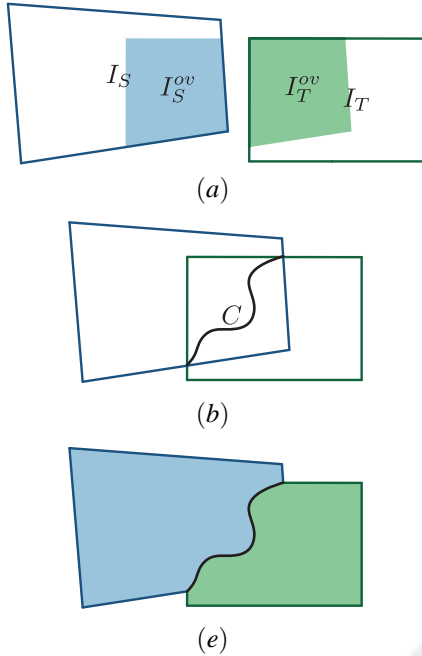


Figure 2: (a) Two registered images and their overlapping area, (b) optimal cutting curve, (c) final stitched images.

Assume we have registered images I_T and I_S . The overlapping area is I_T^{ov} in image I_T and I_S^{ov} in image I_S (as shown in figure 2). We would like to cut and stitch I_T and I_S along an optimal curve C .

Let C be a cutting curve, then the cost of having C as cutting curve is defined as:

$$W(C) = \sum_{p \in C} W(p), \quad (1)$$

where $W(p)$ is the value of the weight function associated with pixel p . The optimal curve(seam) is the curve which minimizes the cost $W(C)$.

Different candidates for weight function are

$$W_g(p) = \|\nabla I_S(p) - \nabla I_T(p)\|_n^n, \quad (2)$$

and

$$W_i(p) = \|I_S(p) - I_T(p)\|_n^n, \quad (3)$$

where $\|\cdot\|_n^n$ is the ℓ_n -norm. A linear combination of $W_g(p)$ and $W_i(p)$ could also be considered as weight function (Jia and Tang, 2005a). We have tested different energy functions and observed that the function

$$W(p) = \|\nabla I_S(p) - \nabla I_T(p)\|_1^1 \quad (4)$$

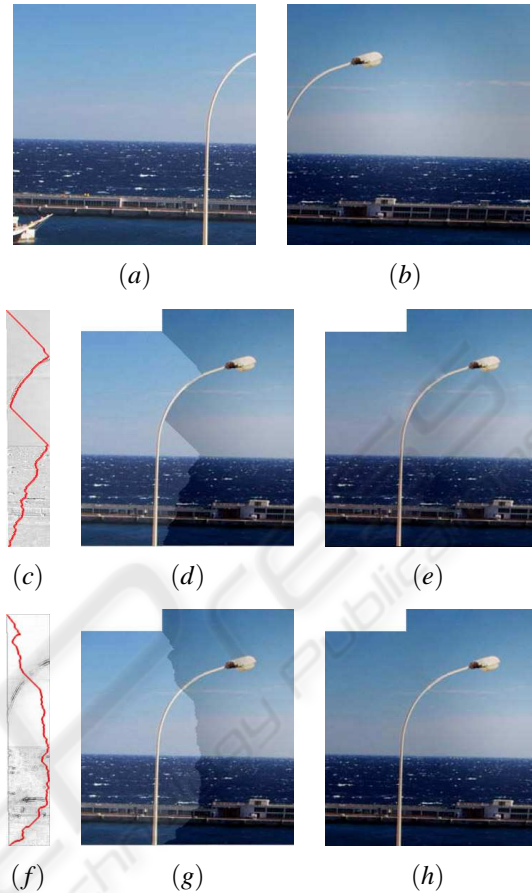


Figure 3: (a) And (b) are the input images. The images are borrowed from figure 6 of (Jia and Tang, 2005a). The images, used in our experiments, are of our size 337×334 . (c) cutting curve using intensity based weight function $W_i(p) = \|I_S(p) - I_T(p)\|_1^1$. (d) Stitching using intensity based weight function without color correction (without PLCC) (e) Stitching using intensity based weight function with color correction (PLCC) (f) cutting curve using gradient based weight function $W_g(p) = \|\nabla I_S(p) - \nabla I_T(p)\|_1^1$. (g) Stitching using gradient based weight function without color correction (without PLCC) (h) Final result after using gradient based weight function and applying PLCC method.

is more reliable than the other candidates specially when the illuminations of I_T and I_S are different. After finding the optimal seam PLCC is applied to correct color and illumination differences between two input images. Setting $n = 1$ (using ℓ_1 -norm) leads to better results because small intensity differences are ignored in higher norms. We use a 3-dimensional RGB color vector for each pixel as $I(p)$, and observed that using HSV color space has the same performance as the RGB color space.

The result of using intensity based weight function and gradient based weight function is shown in Figures 3 and 5.

There are various algorithms with different complexities for finding the optimal cutting curve. Min-Cut(Max-flow) algorithm (Kwatra et al., 2003) works accurately. However due to its high complexity, it imposes significant computational burden on images of high resolution. We used a combination of dynamic programming and BFS (Breadth First Search) algorithm in our experiments to find optimal cutting curve. Its complexity is $O(n)$ where n is the number of pixels in the overlapping area.

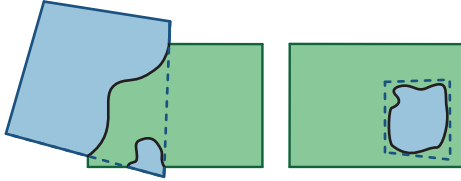


Figure 4: In some cases the optimal seam is not a simple curve.

In some cases the optimal seam gets more complex as shown in Figure 4. Therefore an optimal seam is not necessarily one simple curve.

4 COLOR CORRECTION BASED ON POISSON EQUATION

Poisson equation has been used for image editing and image alignment applications, for example (Pérez et al., 2003), (Jia and Tang, 2005a) and (Agarwala et al., 2004). Here we use Poisson equation to correct color differences between two already registered images.

Lets Ω be the region (in I_S) that lies on one side of the optimal seam (the side belonging to the source image). The boundary of Ω is denoted by $\partial\Omega$. We separate $\partial\Omega$ into two parts: the common boundary with I_T (referred to as $\partial\Omega_C$), and the other boundaries (defined as $\partial\Omega_B$). Our notations are illustrated in Figure 6.

To eliminate artifacts and color differences over the seam $\partial\Omega_C$, we define a correction function Ψ on Ω as

$$\hat{I}_S = I_S + \Psi \quad (5)$$

where \hat{I}_S is the corrected image. Then the Poisson equation is solved on Ω and the resulting correction function Ψ , is added to I_S to compensate for color differences between two images. For colored images, we apply the same method on each color channel of the input image. According to our experiments the performance of the method is the same in RGB and

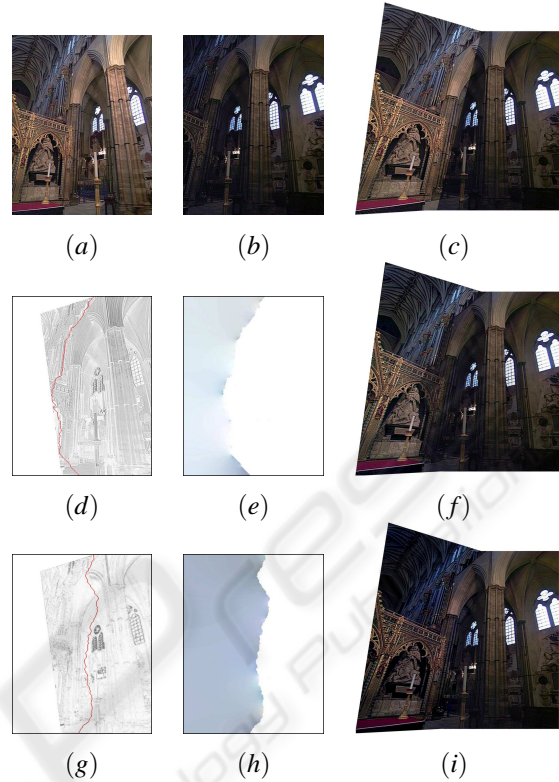


Figure 5: Illustration of applying PLCC on two images. (a) and (b) input images of size 800×600 . (c) the result of putting two registered images together without applying any corrections. (d) a cutting curve found by using intensity based weight function. (e) the solution of the poisson equation solved on the corresponding boundary. (f) the result of stitching the images using an intensity based seam line. (g) shows a cutting curve found using Gradient based weight function. (h) the solution of the poisson equation associated with the cutting curve in (g) and (i) the final result of stitching using intensity based seam line. As you can see, the color is not corrected perfectly in (f) because it's corresponding cutting curve has passed dark areas and the boundary conditions of the poisson equation in (e) is not valid.

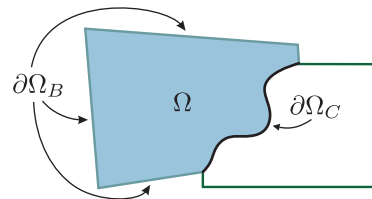


Figure 6: Notation of the region Ω : Ω is the region of the visible part of I_S . The common boundary with I_T is defined as $\partial\Omega_C$, and the other boundaries are defined as $\partial\Omega_B$.

HSV color spaces. For solving Poisson equation on Ω several boundary conditions could be assumed. The

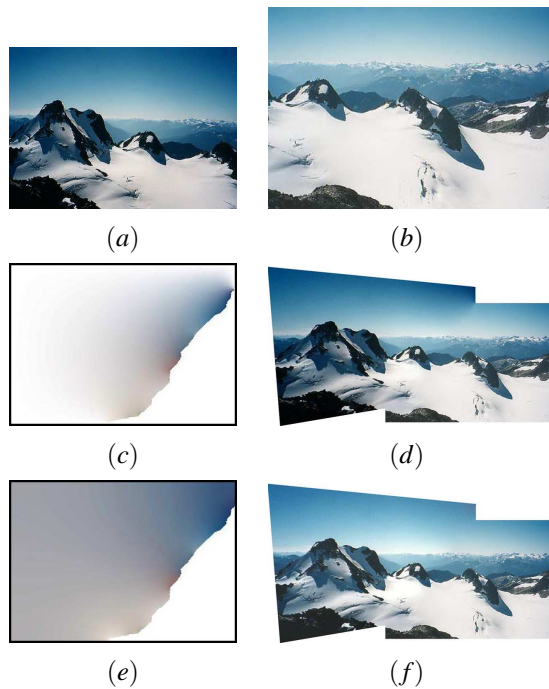


Figure 7: Comparison between the results of using Dirichlet boundary conditions or Neumann boundary conditions on $\partial\Omega_B$. (a) and (b) source and target images, both of size 800×600 . (c) the solution of Poisson equation with Dirichlet boundary conditions on $\partial\Omega_B$ as color correction factor. (d) the respective result of color correction. It is equivalent to applying Poisson image editing (Pérez et al., 2003) (e) the solution of Poisson equation with Neumann boundary conditions on $\partial\Omega_B$ and (f) the result of color correction using the correction factor (e). The correction factor (c) and (e) are solved on a rectangular domain before applying the transformation and added to source images after transformation.

Dirichlet boundary condition equal to the difference between intensity of two input images along $\partial\Omega_C$ was imposed on $\partial\Omega_C$. For $\partial\Omega_B$ the Neumann boundary condition was used.

Imposing the proper boundary condition is critical in our application. One might use Dirichlet boundary condition on $\partial\Omega_B$ (equation 6). However, the problem here is the choice of the boundary function on $\partial\Omega_B$. For the Dirichlet boundary condition, an approximation to the value on $\partial\Omega_B$ is necessary. The trivial approximation zero for the boundary value results in imperfect color correction as shown in Fig. 7.

$$\Delta\Psi = 0 \text{ over } \Omega \text{ with } \begin{cases} \Psi = I_T - I_S, & \text{On } \partial\Omega_C \\ \Psi = \text{Constant}, & \text{On } \partial\Omega_B, \end{cases} \quad (6)$$

where Δ denotes the Laplace operator.

The Neumann boundary condition on $\partial\Omega_B$ in PLCC (equation 7) produced significantly better results. The superior performance of the Neumann boundary condition on $\partial\Omega_B$ is explicable in view of the fact that it does not fix intensity values along $\partial\Omega_B$ but constrains the gradient values along $\partial\Omega_B$ to be zero. Fixing the intensity on $\partial\Omega_B$ results in Ψ to be constant over $\partial\Omega_B$, while the ideal values of Ψ over the $\partial\Omega$ are not necessarily constant. Furthermore, there is no straightforward theoretical way to set the values of Ψ over $\partial\Omega_B$ and an approximation is inevitable. This problem is aggravated where the illumination condition between the input images differ significantly.

$$\Delta\Psi = 0 \text{ over } \Omega \text{ with } \begin{cases} \Psi = I_T - I_S, & \text{On } \partial\Omega_C \\ \frac{\partial\Psi}{\partial n} = 0, & \text{On } \partial\Omega_B, \end{cases} \quad (7)$$

where \hat{n} is normal vector at $\partial\Omega$. This Poisson equation is the result of the following minimization problem (equation 8).

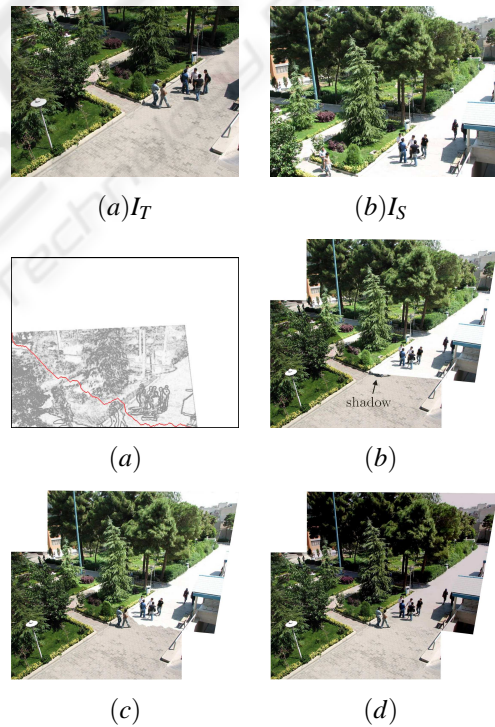


Figure 8: Applying PLCC and optimal seam to dynamic scene. (a) and (b) input images of size 800×600 . (c) Optimal seam based on gradient disparities. (d) Stitching without using optimal seam. The shadow of pedestrians walking behind is visible, while the pedestrians body are eliminated from the stitching result. The color difference is very prominent. (e) Stitching using optimal seam. The shadow of pedestrians are no longer visible. The color differences are still prominent (f) Final result of applying color correction (PLCC) and optimal seam.

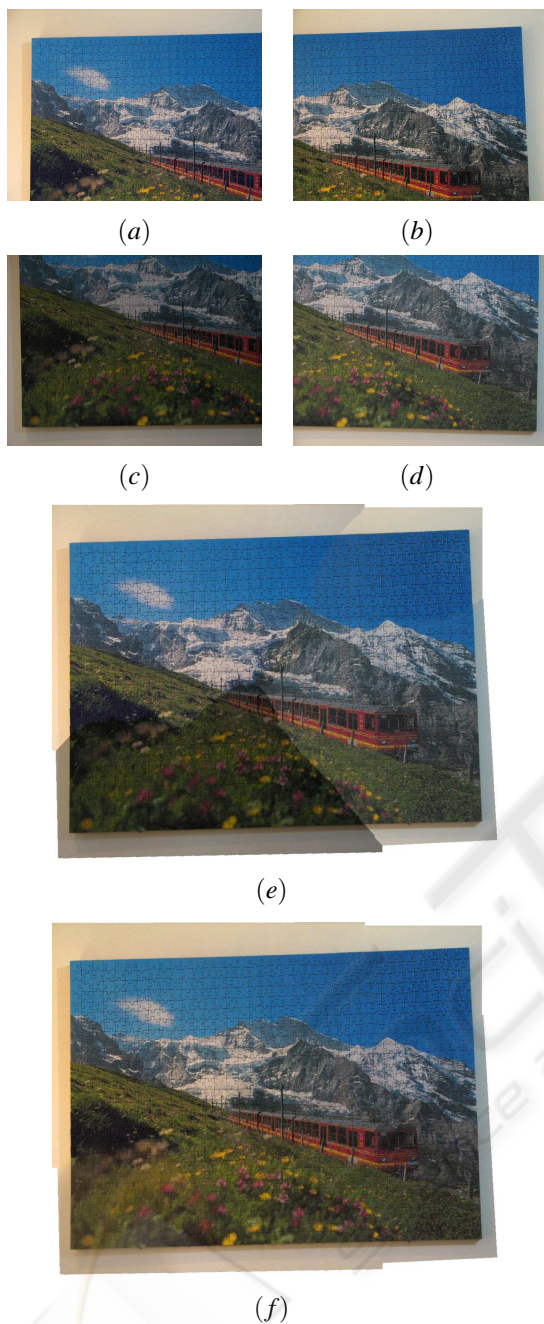


Figure 9: Creating super resolution images using images of poor quality. (a), (b), (c) and (d) are input images (of a puzzle hanged to a wall) taken at four different viewpoints and illumination conditions. input image (a) is taken under yellow light source, (b) taken under yellow and white light sources, (c) taken at low exposure time under white light source and (d) taken under white light source. (e) the stitching result without PLCC. (f) the stitching result after PLCC.

$$\min_{\Psi} \iint_{\Omega} |\nabla \Psi|^2 \text{ with } \begin{cases} \Psi = I_T - I_S, & \text{On } \partial\Omega_C \\ \frac{\partial \Psi}{\partial n} = 0, & \text{On } \partial\Omega_B, \end{cases} \quad (8)$$

where the gradient operator $[\frac{\partial}{\partial x}, \frac{\partial}{\partial y}]$ is represented by ∇ . This minimization problem results in visually natural output images because it minimizes the ℓ_2 -norm of the gradient of intensities near the boundary.

We used the method of finite differences and the central difference formula to solve the Poisson equation and the resulting system of linear equations.

5 EXPERIMENTAL RESULTS

A database for testing and evaluating image stitching algorithms was created. This database contains over two hundred pairs of images from over forty scenes. All pairs are available in three different standard sizes. The scenes vary in color, camera properties, camera location and lighting. The database will be publicly available at "math.ipm.ac.ir/vision". The transformation matrix for each pair of images was determined using (Gheissari et al., 2008). This database contains challenging images for registration, color correction, and building panoramic images.

As mentioned before the optimal seam method is applicable to dynamic scenes. This is because the optimal seam does not pass through areas of high gradient disparity. This capability is shown in figure 8. As can be seen from this figure, two different groups of pedestrians are present in the input images. The optimal seam passes through the narrow gap between these two groups and therefore both groups are presented in the resulting stitched image. If the optimal seam has not been used, then the shadow of the pedestrian group behind would be visible without the pedestrians themselves.

Performance of the proposed method is compared with some standard competing methods. As shown in figure 10, a combination of PLCC and optimal seam outperforms feathering (Uyttendaele et al., 2001), pyramid blending (Adelson et al., 1984), GIST (Levin et al., 2003) and Poisson image editing (Pérez et al., 2003).

The proposed algorithm is desirable for making super resolution images due to its high accuracy and low time complexity. To show this capability we chose four images of a puzzle hanged to a wall. The images were taken at four different view points and significantly various illumination conditions as shown in figure 9. The results of applying the proposed algorithm shows its success .

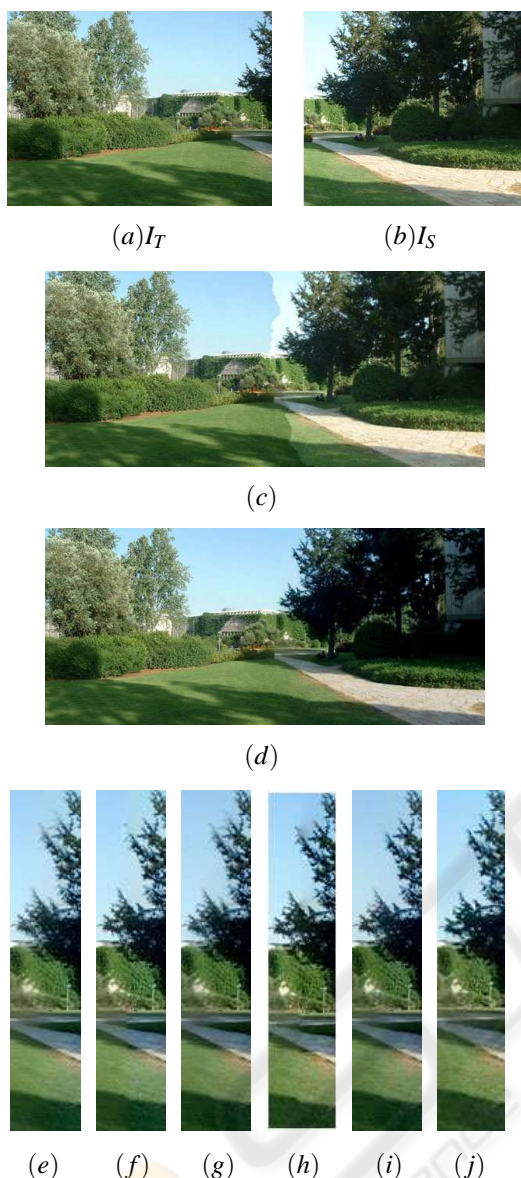


Figure 10: Comparing PLCC with some competing methods: (a) and (b) are input images borrowed from figure 4 of (Levin et al., 2003). The images are of size 348×255 and 290×257 respectively. (c) Stitched image after applying optimal seam, (d) The color correction result generated by PLCC after finding optimal seam, (e) Feathering (Uyttendaele et al., 2001), (f) Pyramid blending (Adelson et al., 1984), (g) Feathering on the gradients (Uyttendaele et al., 2001), (h) Poisson editing (Pérez et al., 2003), (i) GIST (Levin et al., 2003) (j) The result of PLCC method.

6 CONCLUSIONS

A new method for seamless image stitching was presented. The proposed algorithm is a hybrid method, that combines optimal seam approaches and methods

which smooth the intensity transition between two images (by color correction). Using a dynamic programming algorithm, an optimal seam along which gradient disparities are minimized is determined. A local color correction method based on Poisson equation is used to enhance color variations between images. Different boundary conditions to solve the Poisson equation were investigated and tested. We concluded that using mixed boundary conditions generates the most accurate results. To evaluate and compare the proposed method (with some competing methods), a large image database consisting of over two hundred image pairs was utilized. The test image pairs are taken at different lightening conditions, scene geometry and camera positions. Compared to standard methods, proposed approach performed favorably on this database and has shown to be very effective in producing visually acceptable images.

ACKNOWLEDGEMENTS

We would like to acknowledge Dr. Mohammad Reza Mokhtarzade for his valuable advices on solving PDEs. In addition, we would like to acknowledge Dr. Mehrdad Shahshahani for his kind helps in this project and in writing this paper. Mr. Mostafa Kamali Tabrizi helped us in modifying the source code for registration. We appreciate the valuable discussions he had with us. Finally we thank Zohre Sharafi, Parisa Mirshams, Paria Mehrani, Sheyda Beigpoor for providing us with beautiful test images. This project was supported by Institute for studies in theoretical Physics and Mathematics (IPM).

REFERENCES

- Adelson, E. H., Anderson, C. H., Bergen, J. R., Burt, P. J., and Ogden, J. M. (1984). Pyramid methods in image processing. *RCA Engineer*, 29(6).
- Agarwala, A., Dontcheva, M., Agrawala, M., Drucker, S., Colburn, A., Curless, B., Salesin, D., and Cohen, M. (2004). Interactive digital photomontage. *ACM Trans. Graph.*, 23(3):294–302.
- Bozdogan, H. (1987). Model selection and akaike’s information criterion (aic): The general theory and its analytical extensions.
- Burt, P. J. and Adelson, E. H. (1983). A multiresolution spline with application to image mosaics. *ACM Trans. Graph.*, 2(4):217–236.
- Gheissari, N., Tabrizi, M. K., Sharafi, Z., and Mirshams, P. (2008). Model-based global image registration. In *Proc. of the 3rd International Conference on Computer Vision Theory and Applications*, page to appear.

- Hasler, D. and Susstrunk, S. (2000). Colour handling in panoramic photography.
- Jia, J. and Tang, C.-K. (2005a). Eliminating structure and intensity misalignment in image stitching. In *ICCV '05: Proceedings of the Tenth IEEE International Conference on Computer Vision*, pages 1651–1658, Washington, DC, USA. IEEE Computer Society.
- Jia, J. and Tang, M.-C.-K. (2005b). Tensor voting for image correction by global and local intensity alignment. *IEEE Trans. Pattern Anal. Mach. Intell.*, 27(1):36–50.
- Kwatra, V., Schodl, A., Essa, I., Turk, G., and Bobick, A. (2003). Graphcut textures: image and video synthesis using graph cuts. In *SIGGRAPH '03: ACM SIGGRAPH 2003 Papers*, pages 277–286, New York, NY, USA. ACM Press.
- Levin, A., Zomet, A., Peleg, S., and Weiss, Y. (2003). Seamless image stitching in the gradient domain.
- Lowe, D. G. (1999). Object recognition from local scale-invariant features. In *Proc. of the International Conference on Computer Vision ICCV, Corfu*, pages 1150–1157.
- Pérez, P., Gangnet, M., and Blake, A. (2003). Poisson image editing. In *SIGGRAPH '03: ACM SIGGRAPH 2003 Papers*, pages 313–318, New York, NY, USA. ACM Press.
- Shum, H.-Y. and Szeliski, R. (2001). Construction of panoramic image mosaics with global and local alignment. pages 227–268.
- Uyttendaele, M., Eden, A., and Szeliski, R. (2001). Eliminating ghosting and exposure artifacts in image mosaics. pages II–509– II–516 vol.2.

